FORMATION OF AMORPHOUS LANTHANIDE SULFATES AND THEIR CRYSTALLIZATION

AKIRA SAITO

Chemistry Department, Tokyo Gakugei University, Nukui-kita, Koganei, Tokyo 184 (Japan)

ABSTRACT

The sulfate hydrates of trivalent La, Pr, Nd, Sm, Eu and Gd became amorphous anhydrous salts when dehydrated at about 250°C. The rest of the lanthanides and yttrium produced anhydrous salts of cubic structure even at low temperature. The amorphous salts crystallized exothermically when heated to about 400°C. To characterize the amorphous state the heats of crystallization were estimated. They ranged from a few kJ mol^{-1} for La to 40 kJ mol^{-1} for Eu. X-ray diffraction and infrared spectral studies were carried out to find the bonding characteristics of the sulfate anion and the crystal structural variation along the series. In addition isothermal kinetic measurements of dehydration for all the lanthanide and yttrium sulfate hydrates were carried out. Discussions are presented on the mechanism of dehydration in connection with the state of the product phases.

INTRODUCTION

The trivalent lanthanide ions form series of compounds with properties which vary regularly, reflecting the decreasing ionic radii of the cations along the series. Among many oxysalts, the sulfate hydrates are easily obtained as well-grown crystals from aqueous solutions; hence their properties have been studied extensively [1]. Most of the salts are octahydrates of monoclinic structure. Exceptionally, lanthanum sulfate crystallizes as enneahydrate [2] and cerium sulfate octahydrate easily loses some of the water in the air. Although thermal analytical techniques such as DTA, TGA or DSC are easily accessible methods for the study of the thermal properties of solids, thermodynamic interpretation of the results involves many difficulties since the methods provide information of a dynamic nature. Nevertheless, as far as the DTA or TG measurements are made for a series of isostructural or closely related compounds of the cations with systematically varying radii under strictly fixed conditions, it may be possible to extract some correlation between the properties. Thus, all the lanthanide and yttrium sulfate hydrates were reinvestigated by DTA and TGA methods. Typical DTA–TG curves of the lanthanide sulfate octahydrates are shown in Fig. 1. The decomposition
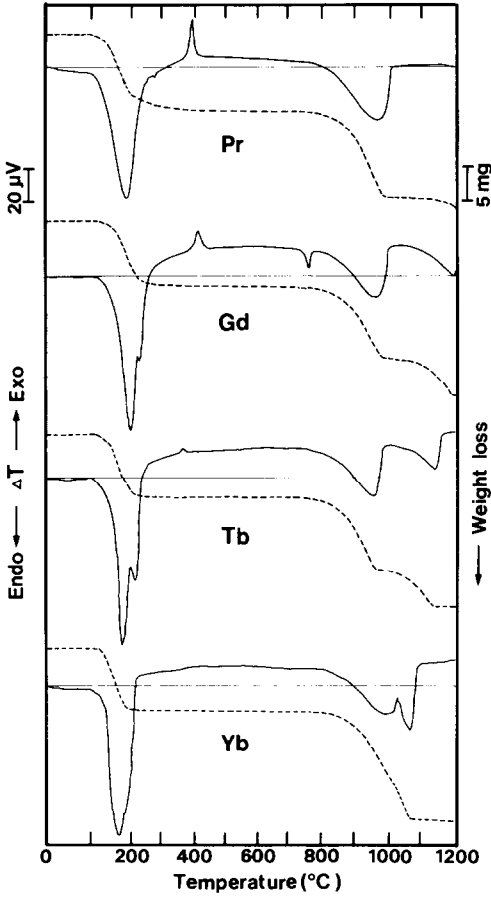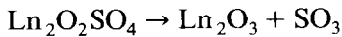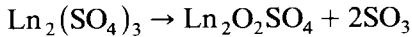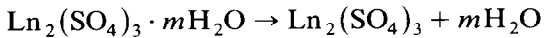
Fig. 1. DTA (solid line) and TG (broken line) curves for the lanthanide sulfate octahydrates: heating rate, $10°C$ min^{-1}; air flow rate, 100 ml min^{-1}; sample amount, 50 mg.

sequence was essentially the same as the data reported by Wendlandt [3,4]. The overall reactions on heating are summarized as follows

$$Ln_2(SO_4)_3 \cdot nH_2O \rightarrow Ln_2(SO_4)_3 \cdot mH_2O + (n-m)H_2O$$

$$Ln_2(SO_4)_3 \cdot mH_2O \rightarrow Ln_2(SO_4)_3 + mH_2O$$

$$Ln_2(SO_4)_3 \rightarrow Ln_2O_2SO_4 + 2SO_3$$

$$Ln_2O_2SO_4 \rightarrow Ln_2O_3 + SO_3$$

However, I observed a few differences which are exemplified by the DTA curve for Gd shown in Fig. 1; it has an exotherm at $350°C$ and an endotherm at $800°C$. Since they are accompanied by no weight change, they must be due to some kind of phase transformation.

The present study thus aimed to elucidate the reasons that the lighter lanthanides show exotherms and the heavier ones do not, and to characterize

the anhydrous sulfates formed on dehydration of the hydrates. To this end, the rate of isothermal dehydration at various temperatures, the heat evolved at the exothermal change, and the powder diffraction patterns of the anhydrous sulfates were measured.

EXPERIMENTAL

Reagents

The rare earth oxides of 99.9% purity were dissolved in a small volume of sulfuric acid. After complete dissolution the solutions were concentrated slowly by evaporation at 40–50°C. Crystalline sulfates formed in the concentrates were filtered with a sintered glass crucible and washed with small amounts of water and then ethanol. The crystals were finally dried in air and stored in a desiccator. The numbers of water molecules for all the hydrates were determined gravimetrically by heating the weighed samples to 400°C.

Thermal analysis

The hydrates were crushed, using an agate mortar, to 100–200 meshes. Samples of 25–50 mg were packed in a platinum crucible of 5 mm diameter and 5 mm height with much care to ensure good reproducibility. DTA and TG curves were obtained simultaneously with a Thermoflex high temperature apparatus (Rigaku Denki Co. Ltd.), from room temperature to 1400°C. Temperatures and temperature differentials were measured by a pair of $Pt + Pt$–13% Rh thermocouples attached to the plates on which the sample and the reference crucibles are placed. As a reference material α-Al_2O_3 was used. Measurements were made in a dynamic atmosphere of air or argon flowing upward around the vertical holder unit at the rate of 100 ml min^{-1}.

Kinetic run of the isothermal dehydration

Isothermal dehydration of the hydrates was followed thermogravimetrically using the same DTA–TG apparatus by holding the furnace temperature constant. Samples were packed in the same way as used in the DTA–TG measurements. Weight loss curves were recorded on the chart until constant weights were attained, with measurements made under dried air flowing at a rate of 100 ml min^{-1}. The empirical activation energies were estimated from the Arrhenius equation.

Infrared spectral and powder X-ray diffraction measurements

A diffractometer equipped with an NaI(Tl) scintillation counter, Model SG-7, Rigaku Denki Co.. was used to measure powder diffraction patterns.

Copper K_α radiation filtered with nickel foil was used. Infrared spectra were recorded on a Model A-3 spectrometer, Japan Spectroscopy Co., employing the KBr disk method.

Estimation of the heat of crystallization

To prepare the anhydrous sulfates of La, Pr, Nd, Sm, Eu and Gd, the respective hydrates were heated at 220–270°C, the lowest temperature at which complete dehydration is accomplished. About 50 mg of the sulfates was used in a single DTA measurement. Conditions such as heating rate, the range of the differential temperature recording and the chart speed were selected to give more reproducible exotherms. Under the same conditions, DTA measurements were made for the standard materials such as $LiNO_3$, $NaNO_3$, KNO_3, $AgNO_3$, and $PbCl_2$ [5]. The heats evolved were estimated by comparing the peak areas with those of the reference materials.

RESULTS

Rates and activation energies of the isothermal dehydration

The isotherms asymptotically approach values for the weights which correspond to the lower hydrates or the anhydrous sulfates. As suggested by the DTA study, some lanthanides tend to form intermediate hydrates with one or two water molecules [3]. In the temperature range studied, the light lanthanides (La–Sm) formed monohydrates, whereas the heavy lanthanides (Er–Lu) and yttrium formed anhydrous salts. For the rest of the lanthanides, the dehydration proceeded to monohydrates at low temperature, and to completion at high temperature. The fractional dehydration α at time t was calculated from the weight changes dW_t and dW_∞ at $t = t$ and $t = \infty$, by the equation $\alpha = dW_t/dW_\infty$. The plot of $1 - (1 - \alpha)^{1/3}$ vs. t gave a straight line at least up to $\alpha = 0.7$–0.9 with the correlation coefficient larger than 0.995, as illustrated in Fig. 2 for Pr, Gd and Lu. This means that the rate-determining step is a phase boundary process, and that as the dehydration proceeds, the hydrate particles, assumed to be spheres with radius r_0, shrink at a constant rate of $dr/dt = k$ [6]. Thus the slope of the straight line is equal to k/r_0 $(= k_L)$, a linear rate constant. Therefore, in order that the observed rate constants are comparable it is required that the sample particles are uniform and their radii are within a limited range for all the lanthanides. Relatively large crystals of the hydrates were crushed with an agate mortar taking much care to produce similar particle size as far as possible. The particle size corresponded to 100–200 mesh, which means that r_0 is in the range from 7×10^{-3} to 4×10^{-3} cm. Since values of k_L are in the order of 10^{-5}–10^{-3} s^{-1}, values of k are in the order of 10^{-7}–10^{-6} cm s^{-1}. The linear
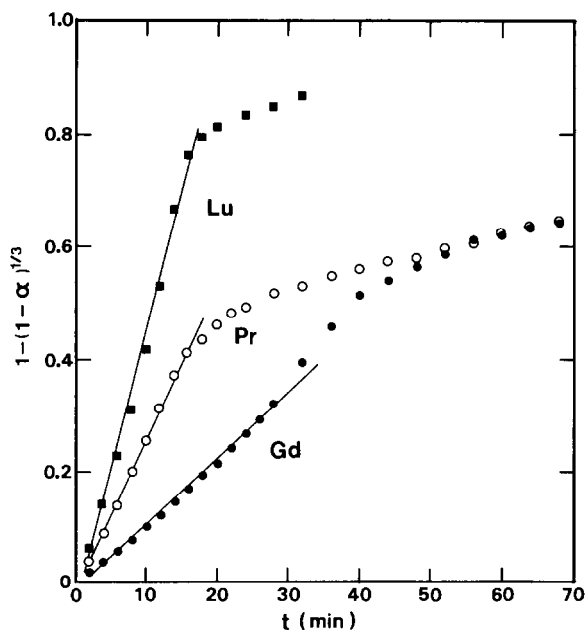
Fig. 2. Plot of $1-(1-\alpha)^{1/3}$ vs. t for the dehydration of sulfate octahydrates at $150\,^{\circ}$C.

rate constants for all the lanthanide and yttrium sulfates obtained at three temperatures are given in Table 1. The empirical activation energies and the pre-exponential factors are also included. In the temperature range studied the linear correlations between $\log k_{L}$ and $1/T$ were quite good. The

TABLE 1

Kinetic parameters for the dehydration of some lanthanide and yttrium sulfate hydrates

|	$k_{L} \times 10^{4}$ (s^{-1})			E_{a} (kJ mol^{-1})	A (s^{-1})
	130°C	150°C	170°C		
La	2.35	5.25	8.11	39.8 $\pm$ 1.8	3.89×10^{1}
Pr	2.00	4.37	8.41	53.3 $\pm$ 1.3	1.63×10^{3}
Nd	1.31	3.35	6.55	59.9 $\pm$ 4.2	7.83×10^{3}
Sm	1.02	2.68	5.34	61.6 $\pm$ 4.4	1.02×10^{4}
Eu	0.733	1.90	5.25	65.7 $\pm$ 1.1	2.43×10^{4}
Gd	0.780	2.01	5.22	70.5 $\pm$ 2.0	1.06×10^{5}
Tb	0.500	2.03	4.71	71.4 $\pm$ 2.7	1.28×10^{5}
Dy	0.782	1.88	4.86	67.8 $\pm$ 3.4	4.72×10^{4}
Ho	0.796	2.47	6.39	69.3 $\pm$ 5.9	8.09×10^{4}
Er	0.856	2.44	6.89	74.2 $\pm$ 0.1	3.49×10^{5}
Tm	0.655	4.28	9.13	84.5 $\pm$ 6.8	9.14×10^{6}
Yb	2.24	5.75	12.0	72.3 $\pm$ 3.1	5.12×10^{5}
Lu	3.06	8.42	15.4	60.2 $\pm$ 7.2	2.05×10^{4}
Y	0.970	1.95	6.73	71.5 $\pm$ 14	1.57×10^{5}
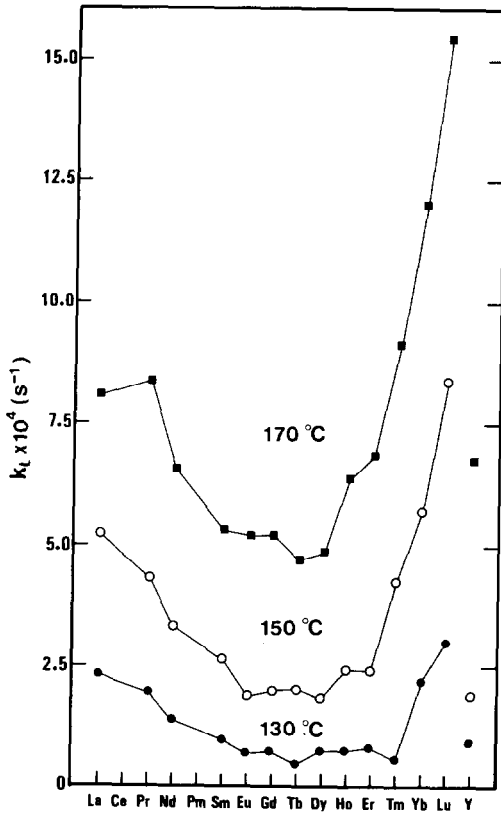
Fig. 3. Linear rate constants (k_L) of the dehydration at 130, 150 and 170 °C.
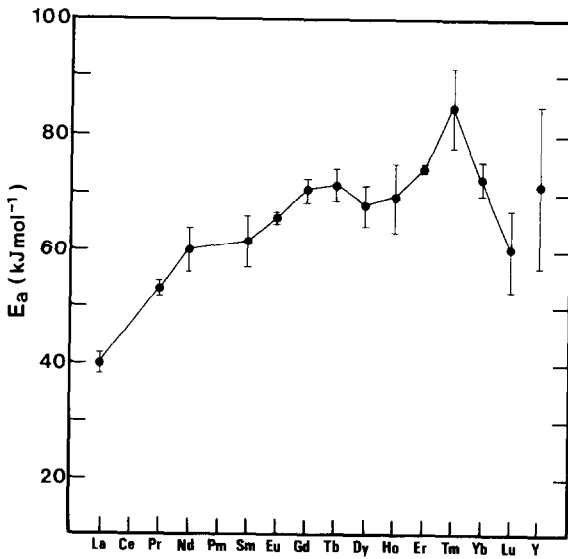

Fig. 4. Activation energies of the dehydration reactions.

standard deviation calculated for the slope applying the least-squares method to the Arrhenius plot is indicated for each point. The rate constants and the activation energies are presented in Figs. 3 and 4 as a function of the atomic number.

Heat and temperature of crystallization

A characteristic feature of the exothermic peak in the DTA curves of the hydrates, as shown in Fig. 1, is that it becomes less apparent with increasing atomic number and is completely missing from the curves for Tm, Yb, Lu and Y. Moreover the peak temperature, T_c, decreases quickly as the atomic number increases after the maximum at Gd, as seen in Fig. 5. These exotherms are assumed to be due to crystallization or modification of the anhydrous sulfates. In fact the X-ray diffraction pattern of the Pr sulfate dehydrated at 250°C for several hours did not show any diffraction lines; on the other hand, the sulfate obtained at 350°C gave a pattern, which showed that the crystallization took place somewhere between the two temperatures. The heats of these transformations estimated for the light lanthanides are included in Fig. 5. The values for Tb to Er is too small to estimate by the method employed here. It is, however, sure that they are much less than the 4 kJ mol^{-1} estimated for La. Many factors influence the reliability of heats estimated by this method. The reproducibility of the DTA run was tested for the standard materials by repeating five times. The
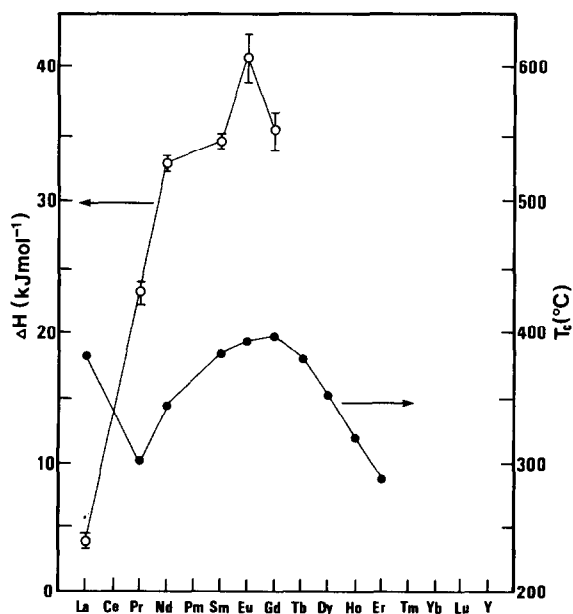

Fig. 5. Peak temperatures (T_c) and heat evolved (ΔH) at the exothermal changes.

standard deviation of the peak areas among them was less than 3%. The most predominant factor is the applicability of the standard materials to the present estimation, since the ratio of peak area to the heat change is a function of the transition temperature. Therefore, I plotted the measured ratios for the standards against their transition temperatures and obtained an extrapolated value at T_c for each lanthanide. Thus, 5–10% uncertainty has to be included in the factors, and accordingly in the estimated heats. The indicated error limits to each point in Fig. 5 stem from only two independent measurements.

DISCUSSION

Mechanism of dehydration

As stated before, k_L is proportional to the rate of shrinking of the sphere, which is constant up to about 40% of the radius of the sphere. This means that the dehydration rate decreases linearly with time. Therefore the probability of escape from the lattice of a water molecule decreases as the reaction proceeds. However, k_L is in the order of 10^{-4} s^{-1}, the probability at an early stage of dehydration is roughly proportional to the rate constant k, i.e., k_L represents the probability of water molecule release from the interface in the initial stages. The variation of k_L with the atomic number shown in Fig. 3 is a result of two cooperative factors; the decreasing $\exp(-E_a/RT)$ with the atomic number and the increasing pre-exponential factor A in the Arrhenius equation $k_L = A \exp(-E_a/RT)$. The activation energies determined here are those for a process in which the interface between the product and the hydrate layers shrinks on dehydration. According to the above discussion, they are related to the energies which are required for a water molecule to be activated in the hydrate lattice, not to diffuse the product layer. It is also noted that the values are almost equivalent to the heats of dehydration, 400–500 kJ mol^{-1} [4], as is generally believed [5]. Since the octahydrates have the same crystal structure, it will be assumed that water molecules are bound in the crystal more strongly for the heavy lanthanides as a result of the smaller cation size: it was observed that activation energies increase with the atomic number.

The pre-exponential factors for solid-phase reactions generally have a wide range of values. Actually the values observed here for the dehydration reactions vary from 10^1 for La to 10^7 for Tm, as given in Table 1. Theoretical estimations have been tried for the thermal decompositions based on the activated complex theory [8–10]. According to this theory, the most significant factor which determines the magnitude of the pre-exponential factor is the degree of rotational freedom of the water molecule in the activated state. That is, the factor is large if the water molecule exists in free

rotational state, and it is small if the molecule is in the restricted rotational state. Since the kinetic data were obtained under specific conditions it is of little value to discuss quantitatively the magnitude of the factor itself; qualitatively, water molecules in the activated state exist as looser complexes for the heavier lanthanides than the lighter ones. This seems to be consistent with the following description of the relationship between dehydration rates and the nature of the product phases of the anhydrous sulfates.

Since the dehydration kinetics were studied under dried air flow, the water vapor pressure in the vicinity of the reacting interface will be sensitively controlled by the diffusivity of water molecules in the product layer. In the amorphous state the released water molecules will interact variously with the disordered ionic constituents: on the other hand, in the crystallized state the interaction will be less because of the compactly organized ions. Moreover the porosity of the latter phase will be larger than that of the former. Thus for the light lanthanide sulfates the low diffusivity brings about higher water vapor pressure, i.e., high impedance to dehydration. The increase in the values of the rate constant with increasing atomic number for the latter half of the series is apparently due to the increasing crystallinity of the product phase (cubic structure).

Formation of the amorphous state and its crystallization

The amorphous sulfates show no diffraction lines, as shown in Fig. 6 for Pr, for example. This kind of diffuse patterns is also exhibited by the solids composed of micro-crystallites. In this case, however, we may regard the amorphous sulfates as being in highly disordered, metastable states which were formed when water molecules were just removed from the original lattice leaving the cations and the anions unarranged in the new phase. This was suggested by the infrared spectra of the amorphous sulfates in which the triply degenerate v_3 and v_4 bands are only weakly split. This means that no coordination of the sulfate ion to a particular cation exists [11]. However, remarkable broadening of the v_3 band may suggest that the anions are surrounded by a strong field produced by the cations. In the hydrates, the water molecules are taking an important role in stabilizing their structures by coordination to the cations and by the hydrogen bond. On the other hand, the major factor which determines the structure of the anhydrous sulfates is the relative size of the lanthanide(III) cations and the sulfate ion. In the crystallized state the sulfate ions are distorted notably from the tetrahedral structure. This is apparent from the infrared spectra of the crystallized forms of Pr and Gd sulfates shown in Fig. 7. It is considered that the lighter lanthanides cannot form geometrically simple structures because of their large ionic radii. Also, Fig. 7 shows that in the cubic structure as for Tb and Yb, the sulfate ions are close to the tetrahedral structure. Thus the crystallization of these amorphous sulfates requires an
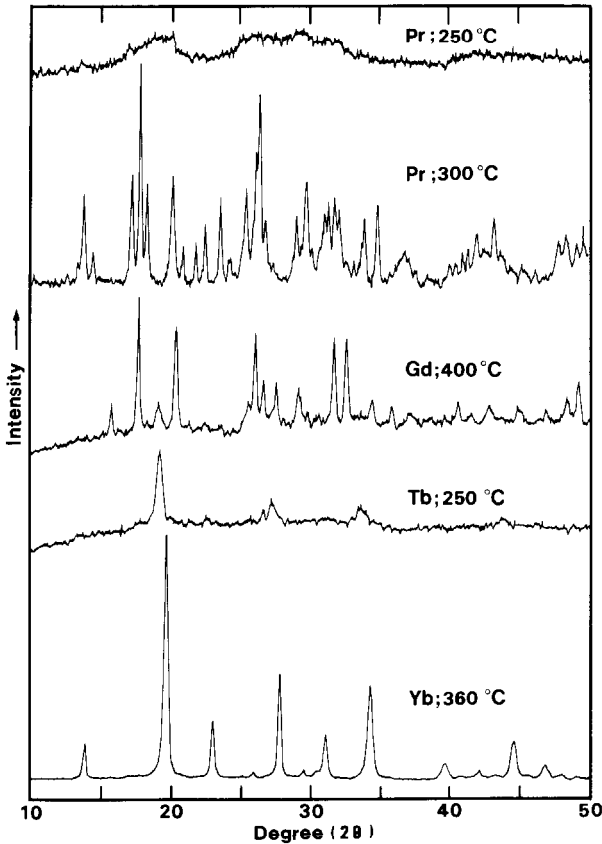
Fig. 6. Powder X-ray diffraction patterns of the lanthanide sulfates dehydrated at the temperatures indicated.

extra amount of energy to cause the distortion of the anions. Consequently they tend to stay in the metastable, amorphous states at low temperatures. Crystallization of the amorphous sulfates begins at a definite temperature nearly 40 °C lower than the peak temperature, T_c, shown in Fig. 5 for the respective lanthanides. The difference between the dehydration and the crystallization temperatures is not larger than 200 K. Therefore the energy of thermal motion of the ions acquired by the temperature elevation amounts to only 2 kJ mol^{-1}. This energy is much less than the excess amount of energy possessed by the amorphous state which is released as heat at crystallization. Frost et al. [12] reported that the high energy amorphous products were produced when some transition metal sulfate hydrates were partially dehydrated in vacuum. They also reported that crystallization was caused at room temperature with the evolution of about 30 kJ mol^{-1}. They discussed the roll of water molecules in the nucleation of the crystallized phase. In the present case, this type of phenomenon was not observed. Only
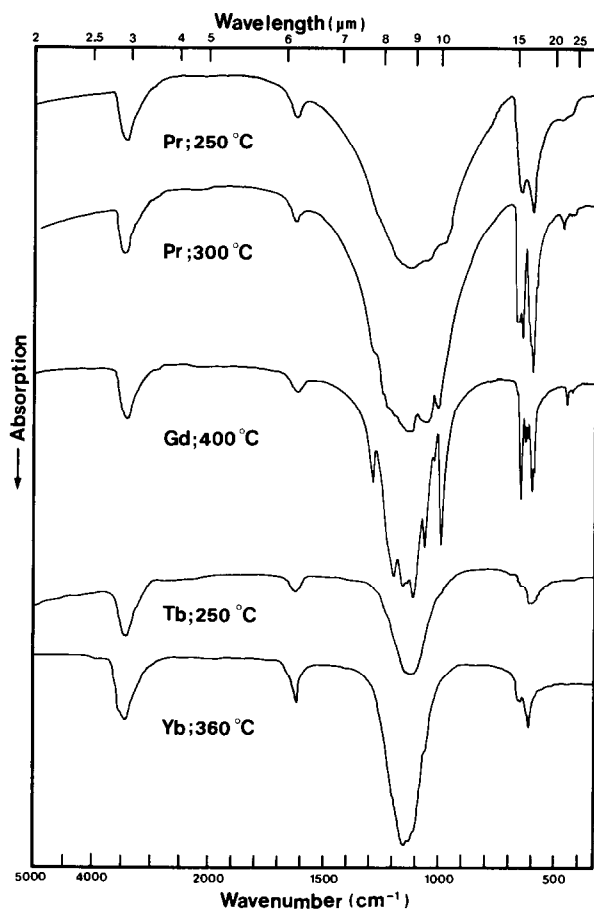
Fig. 7. Infrared spectra of the lanthanide sulfates dehydrated at the temperatures indicated.

the temperature elevation which would increase the mobility of the ions caused the crystallization. Although small exothermic peaks were observed for the DTA curves of Tb to Er, X-ray powder patterns showed no structural change when the sulfates were heated over the corresponding temperatures. Thus they are due to either just a slight modification of the lattice constituents or an improvement of the crystallinity. In fact, some diffraction lines were intensified on heating, more remarkably for heavier lanthanides than the lighter ones. Kinetically the crystallization is composed of two processes, i.e., nucleation and its growth, like the other solid phase reactions. If we define G as the energy required to form a nucleus, the rate of nucleation is proportional to $\exp(-G/T)$ [13]. The temperature T is considered as one at which the rate reaches a definite magnitude and the nucleus formed has a critical size. Hence T_c will be regarded as a measure of the magnitude of G. It is also suggested that a slight modification of the

lattice constituents in the same structural system needs some definite amount of energy, and this energy is larger for phases with a higher degree of disorder. As shown in Fig. 5 and described earlier, Sm, Eu and Gd sulfates are formed on dehydration as those have the largest amount of excess energy, and are in more disordered states than the others. Therefore it is reasonable to consider that more energy is required for nucleation, and that crystallization consistently takes place at the highest temperatures.

Powder diffraction patterns of all the anhydrous sulfates were obtained after being heated at various temperatures. The results show that their crystal structures are quite various. Crystalline sulfates seem to be divided into two groups of the same structure, i.e., La to Eu (refer to A group) and Tb to Lu (B group). Typical patterns of each group are represented by Pr and Yb in Fig. 6. The crystal system of the former is not identified at present, whereas the latter was found to be cubic. Gadolinium sulfate seems to exist in the transient state even at relatively low temperatures, since the pattern seems to include diffraction lines related to both groups. As described earlier, an endothermic peak at 765°C is found in the DTA curve of Gd. The X-ray diffraction measurement found that the endotherm was caused by the phase transition to cubic. The heat of the transformation was roughly estimated to be 20 kJ mol^{-1}. These observations indicate that the crystal system of the A group is stable at low temperatures, and transformation to that of the B group will occur at high temperatures. Actually the endothermic change was also observed for Eu sulfate though it overlapped with the endotherm due to the decomposition to Eu oxysulfate. For the other lanthanides lighter than Eu, the transition temperatures might be much higher than their decomposition temperatures.

REFERENCES

1 T. Moeller, The Lanthanides, in A.F. Trotman-Dickenson (Ed.), Comprehensive Inorganic Chemistry, Vol. 4, Pergamon, Oxford, 1973, pp. 81, 95.
2 E.B. Hunt, Jr., R.E. Rundle and A.J. Stosick, Acta Crystallogr., 7 (1954) 106.
3 W.W. Wendlandt, J. Inorg. Nucl. Chem., 7 (1958) 51.
4 M.W. Nathans and W.W. Wendlandt, J. Inorg. Nucl. Chem., 24 (1962) 869.
5 C. Duval, Thermal Methods in Analytical Chemistry, in G. Svehla (Ed.), Comprehensive Analytical Chemistry, Vol. VII, Elsevier, Amsterdam, 1976, p. 131.
6 P.W.M. Jacobs and F.C. Tompkins, Classification of the Solid Reactions, in W.E. Garner (Ed.), Chemistry of the Solid State, Butterworth, London, 1955, p. 201.
7 W.E. Garner, The Kinetics of Endothermic Solid Reactions in W.E. Garner (Ed.), Chemistry of the Solid State, Butterworth, London, 1955, p. 221.
8 R.D. Schultz and A.O. Dekker, J. Phys. Chem., 60 (1956) 1095.
9 R.D. Shannon, Trans. Faraday Soc., 60 (1964) 1902.
10 H.F. Cordes, J. Phys. Chem., 72 (1968) 2185.
11 K. Nakamoto, Infrared and Raman Spectra of Inorganic and Coordination Compounds, 3rd edn., Wiley, New York, 1978, p. 197.
12 G.B. Frost, K.A. Moon and E.H. Tompkins, Can. J. Chem., 29 (1951) 604.
13 A.R. West, Solid State Chemistry and its Applications, Wiley, New York, 1984, p. 438.